Int J Thermophys (2012) 33:1778–1786
DOI 10.1007/s10765-012-1322-x

Detection of Dental Secondary Caries Using Frequency-Domain Infrared Photothermal Radiometry (PTR) and Modulated Luminescence (LUM)

J. Kim · A. Mandelis · A. Matvienko · S. Abrams · B. T. Amaechi

Received: 10 February 2012 / Accepted: 24 September 2012 / Published online: 7 October 2012

Abstract The ability of frequency-domain photothermal radiometry (PTR) and modulated luminescence (LUM) to detect secondary caries is presented. Signal behavior upon sequential demineralization and remineralization of a spot (diameter ∼1 mm) on a vertical wall of sectioned tooth samples was investigated experimentally. From these studies, it was found that PTR–LUM signals change, showing a certain pattern upon progressive demineralization and remineralization. PTR amplitudes slightly decreased upon progressive demineralization and slightly increased upon subsequent remineralization. The PTR phase increased during both demineralization and remineralization. LUM amplitudes exhibit a decreasing trend at excitation/probe distances larger than 200 μm away from the edge for both demineralization and remineralization; however, at locations close to the edge (up to ∼200 μm), LUM signals slightly decrease upon demineralization and slightly increase during subsequent remineralization.

J. Kim (✉) · A. Mandelis · A. Matvienko
Department of Mechanical and Industrial Engineering, Center for Advanced Diffusion-Wave Technologies, University of Toronto, 5 King's College Road, Toronto, ON M5S 3G8, Canada
e-mail: daedjungho@gmail.com

J. Kim
194 Maplehurst Ave., Toronto, ON M2N 3C2, Canada

A. Mandelis · S. Abrams
Quantum Dental Technologies Inc., 748 Briar Hill Ave, Toronto, ON M6B 1L3, Canada

B.T. Amaechi
Department of Comprehensive Dentistry, University of Texas Health Science Center at San Antonio, 7703 Floyd Curl Drive, San Antonio, TX 78229-3900, USA

Keywords Caries · Demineralization · Luminescence · Photothermal radiometry · Remineralization · Secondary caries · Wall lesions

1 Introduction

Dental secondary caries is the carious lesion developed between the marginal interface of an existing restoration and a tooth [1,2], and it is the principal cause of restoration replacement [3–10]. As secondary caries occurs at subsurface regions that are not externally visible in most cases, a novel non-destructive technology to detect dental secondary caries has become highly desirable. Current detection methods, including visual inspection and radiography, are not able to image or detect caries in these areas at early phases of the caries process [11–16]. The photothermal radiometry–modulated luminescence (PTR–LUM) technique was developed as a caries detection tool, and its ability to detect various types of dental caries and defects was proven by many studies [17–23]. In this report, studies of the ability of the PTR–LUM technique to detect artificially developed dental secondary caries are presented.

2 Experimental Apparatus and Procedures

2.1 Sample Preparation

Several extracted human molar teeth free of cracks, stains, brown spots, or white spots were collected from oral surgeons. The teeth were stored in distilled water until they were vertically sectioned in half with a diamond-tipped cutter ensuring that the natural side surfaces of the teeth remained intact. Each half tooth was mounted on a LEGO block (Fig. 1a). In total, four samples were prepared and stored in a humid container to prevent dehydration until they were used for treatments and PTR–LUM scans.

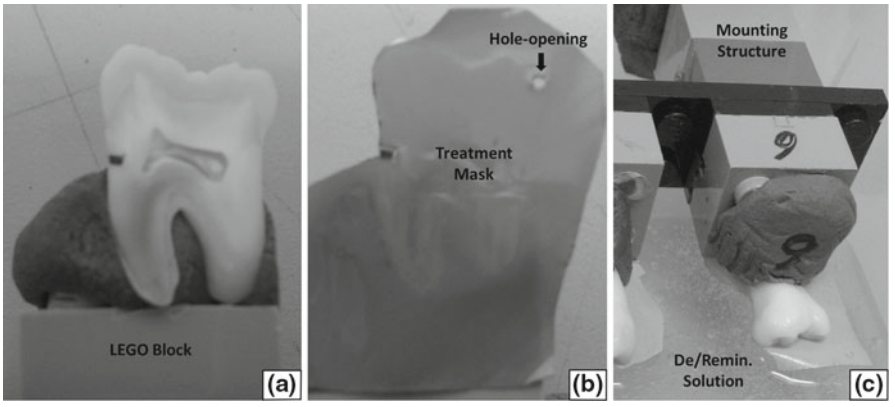

Fig. 1 (a) Sample structure: a vertically sectioned tooth sample was mounted on a LEGO block; (b) plastic tape with a hole (opening) was attached to the vertical surface of the tooth sample before each demineralization/remineralization step; and (c) sample was mounted on a supporting structure inside the treatment cell containing either a demineralization or remineralization solution

2.2 Demineralization/Remineralization of the Sample

The samples were artificially demineralized to mimic natural secondary caries, and followed by artificial remineralization. Before each demineralization or remineralization treatment, an adhesive plastic tape (colored UPVC tape, 3M) with a hole (opening) was attached to the sectioned vertical surface of the sample (Fig. 1b). Then the sample was fixed to the mounting structure inside the treatment cell (Fig. 1c), which allows only the perforated area of the vertical surface of the sample to be treated by either a demineralization or a remineralization solution. After each treatment, the sample was removed from the cell, the masking tape was removed, and the sample was cleaned with flowing tap water to dispose of any remaining solution and adhesives from the masking tape. An acidified gel-type solution (pH 4.5) was used for demineralization, which was composed of 0.1 M lactic acid ($C_3H_6O_3$), 0.1 M NaOH, and 14 % w/v hydroxyethyl cellulose. Artificial saliva (pH 7.0) was used for subsequent remineralization, and its chemical composition was 0.3542 g $Ca(NO_3)_2$, 0.1225 g KH_2PO_4, 9.692 g KCl, and 4.28 g cacodylic acid ($C_2H_7AsO_2$).

2.3 Principle of the Technique

PTR is based on the modulated photothermal response of a medium. When the optical energy from a modulated excitation source is absorbed by a medium, non-radiative optical-to-thermal energy conversion occurs which results in a modulated temperature and can be monitored by an infrared detector. The PTR signals contain subsurface information in the form of a spatially damped temperature depth integral; therefore, it is possible to do photothermal depth profiling of the interrogated medium using PTR [24]. LUM is based on the optical-to-radiative energy conversion. Absorption of the optical energy from the laser source results in excitation of chromophores to a higher energy state followed by de-excitation to a lower energy (ground) state and emission of longer wavelength photons. This longer wavelength signal constitutes LUM which can be detected by a photodetector. However, LUM signals can also include, or even be dominated by, laser light reflected or back-scattered by a turbid sample. This back-scattered light can be filtered out by placing an optical filter in front of the photodetector; however, the closeness of excitation and LUM wavelengths often makes it difficult to fully filter out laser contributions to the detected LUM signal.

2.4 Apparatus

A semiconductor laser diode with a wavelength of 660 nm and maximum power of 130 mW was used as an excitation source (Opnext, HL6545MG). A laser diode controller (Thorlabs, LDC202B) triggered by the software lock-in amplifier (National Instruments, NI6221) modulated the laser current. The modulated laser beam was focused on the tooth surface with the aid of lenses (Thorlabs, LMR1). The modulated PTR response emitted from the photoexcited tooth was focused by two off-axis paraboloidal mirrors and collected by the mid-infrared HgCdZnTe (MCZT) detector (VIGO, PVI-2TE-5). The LUM response was focused onto a photodetector (Thorlabs,

PDA36A). A cut-on colored glass filter (cut-on wavelength of 715 nm, Edmund Optics) was placed in front of the photodetector to block unwanted laser light reflected or scattered by the tooth. Collected PTR–LUM signals were digitized and stored using the software lock-in amplifier and Labview software.

2.5 Experimental Procedures

PTR–LUM scans were conducted at several stages of demineralization followed by remineralization: before demineralization, after demineralization of (1, 2, 3, 5, 7, 10, and 14) days, and after remineralization of (1, 2, 3, 4, and 6) weeks. Two types of PTR–LUM scans were conducted, which include line scans and frequency scans. Line scans were measured by PTR–LUM along a spatial coordinate on the tooth surface at fixed frequencies: 2 Hz and 200 Hz for PTR and LUM, respectively. Each line scan was conducted along a line on the side surface of the tooth sample perpendicular to the sectioned vertical wall, as indicated with a dotted arrow in Fig. 2a. The measurement was started from the interfacial edge of the tooth sample and moved in the direction of the dotted arrow. The micrometer stage on which the tooth sample was placed, was adjusted accordingly after each measurement. After each change of position, a 15 s time delay was allowed for signal stabilization. Frequency scans were performed at some fixed positions on the side surface of the sectioned tooth to examine the frequency dependence of PTR–LUM: at the vertical edge (Fig. 2a), 200 μm and 2 mm away from the edge. Four frequencies were used for the scans: (2, 6, 15, and 200) Hz. Each scan was started at 2 Hz, and the frequency was automatically increased after measurements were taken at one frequency using Labview software. After each frequency change, a 15 s time delay was allowed for signal stabilization.

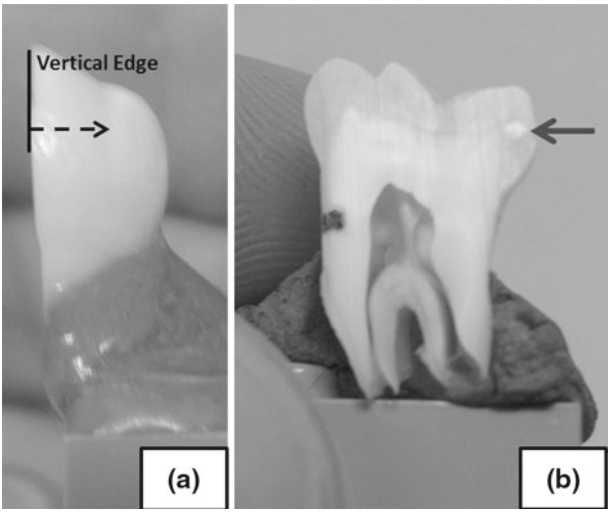

Fig. 2 (a) Side surface of a sample on which PTR–LUM line and frequency scans were conducted and (b) white spot was created at the top right corner of the vertical surface of a tooth sample after 1 day of demineralization (indicated with a *solid arrow*)

3 Results and Discussion

Figure 2b clearly shows that a white spot was created at the top right corner of the vertical wall even after 1 day of demineralization. It indicates that demineralization actually occurred and made physical changes to the sample. Figures 3 and 4 show line- and frequency-scan results of one representative sample (sample 1), respectively. PTR–LUM plots at some treatment stages are omitted, as it may be hard to distinguish from one curve to another with all the data crowded. Figure 3 shows that PTR amplitudes exhibit a slightly decreasing trend upon progressive demineralization, and a reversal, slight increases upon subsequent remineralization. The PTR phase shows an increasing trend during both de- and remineralization although the trend was non-monotonic with treatment time. This non-monotonic temporal behavior of PTR signals is consistent with other observations involving demineralization of uncut (whole) dental enamel surfaces using the same gel [23,24]. It appears that the state of the demineralization of the vertical wall follows similar trends and the PTR signal is controlled by wall demineralization processes, as expected. LUM amplitudes exhibit a decreasing trend at excitation/probe distances larger than ~200 μm away from the edge for both de- and remineralization; however, at locations close to the edge (up to ~200 μm),

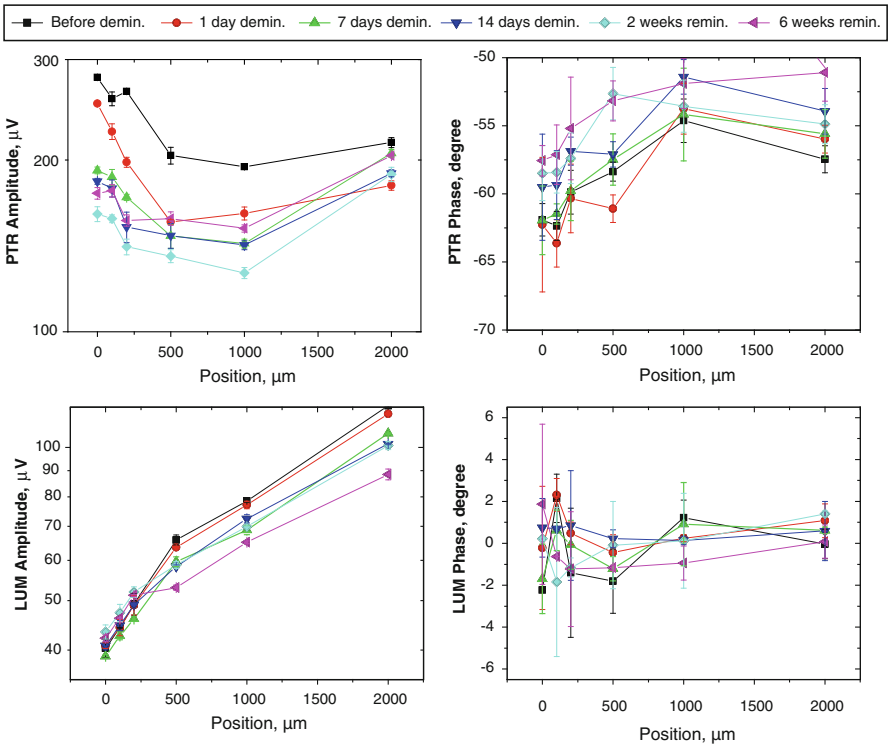

Fig. 3 PTR-LUM line scan results of sample 1 upon progressive demineralization and remineralization: PTR signals were collected at 2 Hz, and LUM signals were collected at 200 Hz for better signal-to-noise ratio

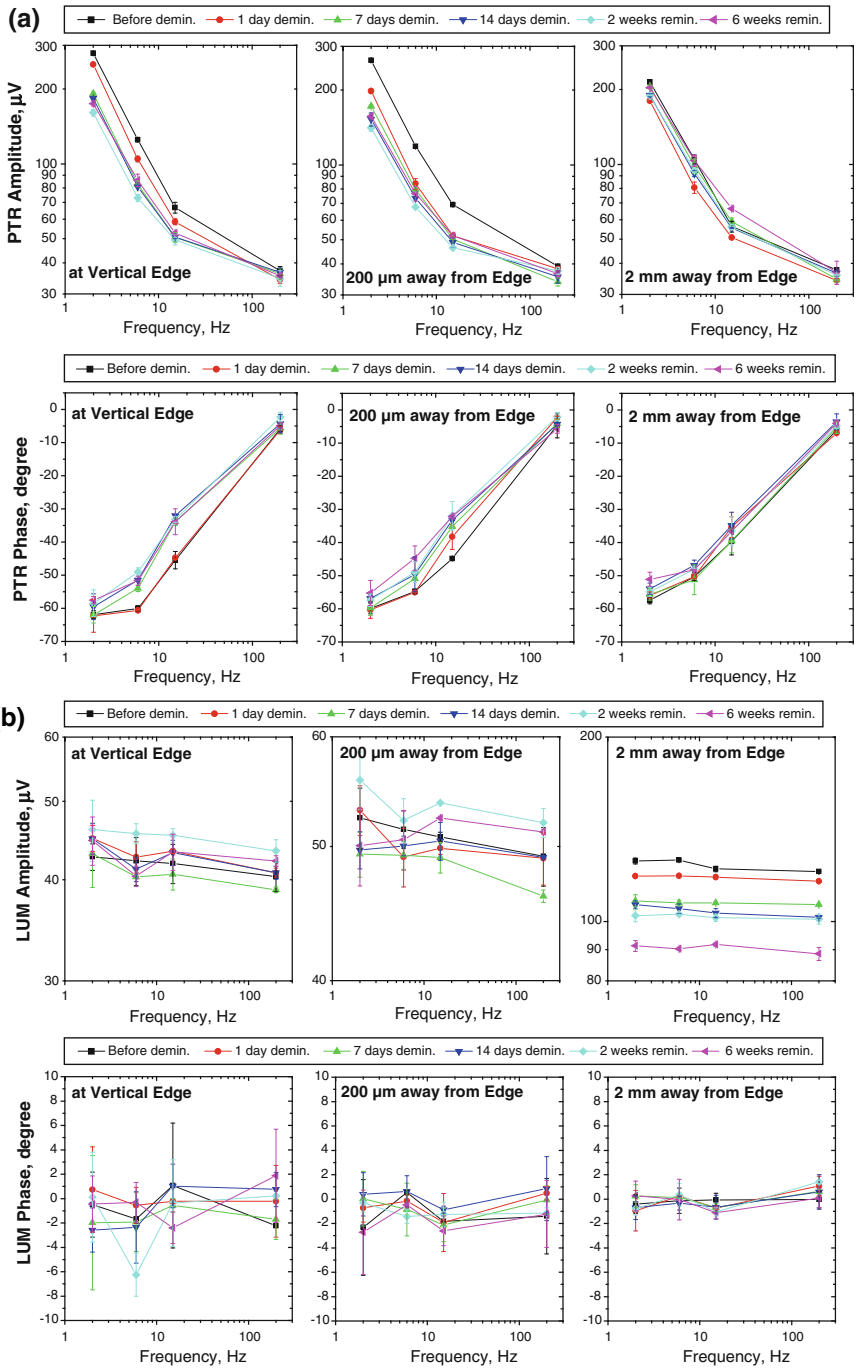

Fig. 4 (a) PTR and (b) LUM frequency scan results of sample 1 upon progressive demineralization and remineralization measured at three different locations on the side surface of the sample: at the vertical edge, 200 μm away from the vertical edge, and 2 mm away from the vertical edge.

Table 1 PTR–LUM scan results at a fixed position (200 μm away from the vertical edge) after each demineralization and remineralization period with ±error shown for each signal channel

Treatment	PTR		LUM	
	Amplitude (μV)	Phase (°)	Amplitude (μV)	Phase (°)
Demineralization				
Before treatment	263.882	−59.883	49.198	−1.407
1 day	198.185	−60.335	49.012	0.475
2 days	177.570	−61.040	48.452	−0.083
3 days	232.331	−58.853	45.896	−0.337
5 days	167.465	−59.885	46.872	−0.189
7 days	172.012	−59.776	46.032	−0.072
10 days	161.917	−59.443	45.083	−0.857
14 days	152.699	−56.867	49.098	0.853
Remineralization				
1 week	147.809	−56.380	49.800	−0.145
2 weeks	140.940	−57.399	52.006	−1.157
3 weeks	134.538	−58.911	49.393	0.740
4 weeks	136.372	−57.039	52.725	−0.120
6 weeks	156.727	−55.202	51.221	−1.230
±Error for each channel[c]	4.386	2.091	1.163	1.417

PTR amplitude and phase signals were measured at a frequency of 2 Hz
LUM amplitude and phase signals were measured at a frequency of 200 Hz
±Error is obtained as an average standard deviation value of each channel during measurements

LUM signals slightly decrease upon demineralization and slightly increase during the subsequent remineralization. Hellen et al. [25,26] conducted some studies using whole tooth samples treated on their outer enamel surfaces from which PTR–LUM measurements were taken directly. They found that PTR amplitudes increased and LUM amplitudes decreased with demineralization as the generated microporosities on the demineralized layer resulted in higher optical scattering coefficients. The same concept of microporosities can be applied to this study where decreasing amplitudes of both PTR and LUM upon demineralization can be explained by hypothesizing that loss of minerals due to demineralization results in an increased loss of photons across the vertical wall. Figure 4a, b shows that frequency-scan results of the same sample exhibit the same trend as the line-scan result in Fig. 3. It also shows that PTR frequency-scans in Fig. 4a converge above 100 Hz, indicating that they become less sensitive, or even insensitive, to the boundary condition of the vertical wall when the decreasing thermal diffusion length centered at the location of the laser beam does not reach the vertical wall. The thermal diffusion length μ_{th} can be calculated from its definition, $\mu_{\text{th}}\ f = (\alpha/\pi f)^{0.5}$, where α is the sample thermal diffusivity and f is the laser modulation frequency. This thermal parameter is inversely proportional to the square root of frequency. Table 1 shows the PTR–LUM signals at a fixed position (200 μm away from the edge) numerically. The ±error for each channel is also shown

in the table. From the table, it is clearly seen that even after 1 day of demineralization, the PTR amplitude decreased much beyond the error bar, which makes sense considering that a white spot was created even after 1 day of demineralization as shown in Fig. 2b. The PTR phase also changed, but the amount of change with respect to the error bar was lower than the PTR amplitude. The LUM amplitude changed beyond the error bar after 3 days of demineralization; however, the amount of changes of the PTR amplitude after each demineralization was much larger than that of the LUM amplitude. This indicates that PTR is more sensitive to demineralization. Signal changes due to remineralization of all channels (excluding the noisy LUM phase due to the weak signal strength) were generally moderate compared to demineralization.

4 Conclusion

PTR amplitudes decreased upon demineralization and increased upon remineralization of the sectioned vertical wall; the PTR phase increased with both de- and remineralization; and LUM amplitudes decreased with demineralization while exhibiting enhanced sensitivity to remineralization at probe locations close to the vertical wall. These trends show that de- and remineralization on the vertical wall of tooth samples greatly affected PTR–LUM and these methods can be used, in turn, to monitor wall lesions.

Acknowledgments This work was supported by The Health Technology Exchange (HTX) and the 2007 (Inaugural) Ontario Premier's Award in Science and Technology to AM.

References

1. I.A. Mjor, F. Toffenetti, Quintessence Int. **31**, 165 (2000)
2. E.A. Kidd, J. Dent. Educ. **65**, 997 (2001)
3. I.A. Mjor, Oper. Dent. **6**, 49 (1981)
4. L.H. Klausner, G.T. Charbeneau, J. Mich. Dent. Assoc. **6**(7), 249 (1985)
5. J. Qvist, V. Qvist, I.A. Mjor, Acta Odontol. Scand. **48**, 297 (1990)
6. I.A. Mjor, F. Toffenetti, Oper. Dent. **17**, 70, 82 (1992)
7. I.A. Mjor, C.M. Um, Int. Dent. J. **43**, 311 (1993)
8. I.A. Mjor, Acta Odontol. Scand. **55**, 58 (1997)
9. F.E. Pink, N.J. Minden, S. Simmonds, Oper. Dent. **19**, 127 (1994)
10. K.H. Friedl, K.A. Hiller, G. Schwartz, Oper. Dent. **19**, 228 (1994)
11. M.J. Tyas, Aust. Dent. J. **36**, 236 (1991)
12. E.A. Kidd, D. Beighton, J. Dent. Res. **75**, 1942 (1996)
13. L.A.F. Pimenta, N.M.F. Lima, A. Consolaro, J. Prosthet. Dent. **74**, 219 (1995)
14. A. Zoellner, B. Diemer, H.P. Weber, A. Stassinakis, P. Gaengler, J. Prosthet. Dent. **88**, 54 (2002)
15. J. Bader, J. Evid. Based Dent. Pract. **3**, 90 (2003)
16. P.A. Mileman, W.B. Hout, Dentomaxillofac. Radiol. **31**, 7 (2002)
17. L. Nicolaides, A. Mandelis, S.H. Abrams, J. Biomed. Opt. **5**, 31 (2000)
18. R.J. Jeon, A. Mandelis, S.H. Abrams, Rev. Sci. Instrum. **74**, 380 (2003)
19. R.J. Jeon, C. Han, A. Mandelis, V. Sanchez, S.H. Abrams, Caries Res. **38**, 497 (2004)
20. R.J. Jeon, A. Mandelis, V. Sanchez, S.H. Abrams, J. Biomed. Opt. **9**, 804 (2004)
21. R.J. Jeon, A. Matvienko, A. Mandelis, S.H. Abrams, B.T. Amaechi, G. Kullkarni, J. Biomed. Opt. **12**, 034028 (2007)
22. R.J. Jeon, A. Hellen, A. Matvienko, A. Mandelis, J. Biomed. Opt. **13**, 034025 (2008)

23. R.J. Jeon, K. Sivagurunathan, J. Garcia, A. Matvienko, A. Mandelis, S.H. Abrams, J. Phys. Conf. Ser. **214**, 012023 (2010)
24. M. Munidasa, A. Mandelis, in *Principles and Perspectives of Photothermal and Photoacoustic Phenomena*, vol. 1, ed. by A. Mandelis (Elsevier, New York), pp. 299–367
25. A. Hellen, A. Mandelis, Y. Finer, B.T. Amaechi, J. Biomed. Opt. **16**, 071406 (2011)
26. A. Hellen, M.S. Thesis, University of Toronto (2010)